Appendix B. Experimental schematic and circuit diagrams for the vibrating orifice aerosol generator and the high-speed, high-voltage switch employed in the dynamics experiment

B.1. Introduction

Field induced droplet ionization mass spectrometry (FIDI-MS) is a useful technique with applications to chemical and biological analysis, but many questions remain regarding the chemistry and physics of the process. This appendix serves to more rigorously cover the experimental details of the FIDI dynamics experiment recently published.[1] The vibrating orifice aerosol generator (VOAG) and electronic circuits are presented and discussed in detail. Pertinent design considerations and safety requirements are discussed in the context of designing future dynamics and mass spectrometric applications for field-induced droplet ionization.

Figure B.1 shows a schematic representation of the hardware employed for the study of FIDI dynamics presented in Chapter 7.[1] Briefly, a vibrating orifice aerosol generator breaks a stream of methanol into monodisperse droplets. These droplets pass between two plates that establish a switched high electric field with custom electronics. All of this hardware was produced in-house and discussed below. Section B.2 illustrates
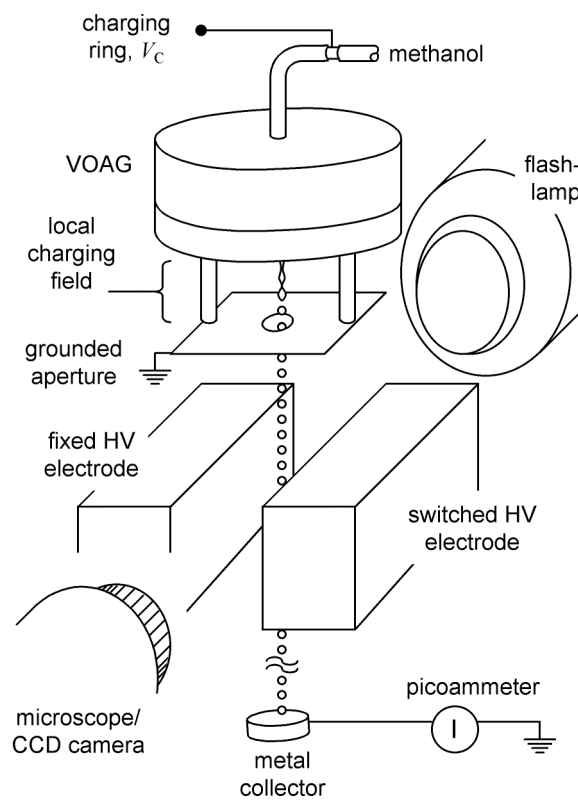
Figure B.1. Schematic of the experimental apparatus employed for the dynamics experiment presented in Chapter 7. Details of the construction of the vibrating orifice aerosol generator are discussed in section B.2. Electronic schematics for the high voltage switching circuit are presented in section B.3. Reprinted from Grimm and Beauchamp.[1]

the design of the VOAG. Section B.3 presents the schematic diagram of the electronic circuits that control the switched electric fields in the experiment. Lastly, section B.4 discusses the considerations and constraints for designing future experiments.

B.2. Vibrating orifice aerosol generator for the dynamics experiment

Vibrating capillary and vibrating orifice aerosol generators produce highly monodisperse liquid aerosols in the micron size range. A brief review by Chen and John details the technique and physics behind this method of aerosol generation.[2] Our VOAG is an in-house design that employs an annular piezoelectric crystal to vibrate a ceramic nozzle.

B.2.1. Aerosol generator design

Capillary instability dictates that the liquid stream exiting the ceramic nozzle will break into droplets at a natural frequency determined by the stream diameter, speed, and surface tension. Without an external influence this breakup is unstable and leads to broad distribution in droplet sizes. When the droplets exit an orifice vibrating at the natural breakup frequency, the superposition vibrations result in steady breakup and monodisperse droplets.

Figure B.2 shows both perspective (A) and cutaway (B) views of the VOAG source. A 1/32 inch inner diameter, 3/32 inch outer diameter silicone tube serves as the sample line that delivers methanol to the VOAG. Liquid is delivered to the sample line from a 500 mL methanol reservoir under ~1-3 psig pressure. This nitrogen backing provides less control but a more steady flow than a syringe pump. Because droplet size is

dependent on flow rate, a steady flow is critical to the formation of monodisperse droplets.

A 130 μm I.D. ceramic orifice (4P480-0016-343; Kulicke and Soffa Inc., Willow Grove, PA) is connected to the end of the sample line. The ceramic tip has a 1/16 inch O.D. at the non-orifice side which creates a tight seal with the 1/32 inch I.D. silicone without the need for further clamping or sealing. Smooth flow through the orifice is critical for monodisperse droplet generation with a minimum of satellite droplets. The stability is verified by observing the flow of methanol through the orifice when removed from the VOAG.

The VOAG head consists of a piezoelectric actuator mounted between a piece of Delrin and aluminum. The annular piezoelectric element is 1/4 inch tall with a 1 inch O.D. and a 5/8 inch I.D. The actuator sits in a circular piece of Delrin machined into an upside-down "hat" shape. The actuator is held into place by a disk of aluminum that is 1/8 inch thick. The Delrin hat is mounted to a piece of Teflon on a three-dimensional translation stage that allows precise alignment of the droplet stream relative to the high field region.

The piezo actuator axially expands and contracts imparting a vibration to the entire VOAG head. A 3/32 inch diameter hole though the Delrin and aluminum allows the sample line and ceramic orifice to be positioned inside the VOAG head. The slight expansion of the silicone tubing around the ceramic allows for good mechanical contact with the VOAG head so that the mechanical oscillations are transferred to the orifice. Piezoelectric action is initiated by the application of a square wave to the piezo element.

A

B

Sample line

Teflon mount

Delrin "hat" cut to fit
inside piezo element

1/8" O.D. 5/8" I.D.
1/4" thick piezo element

1/8" thick aluminum disk
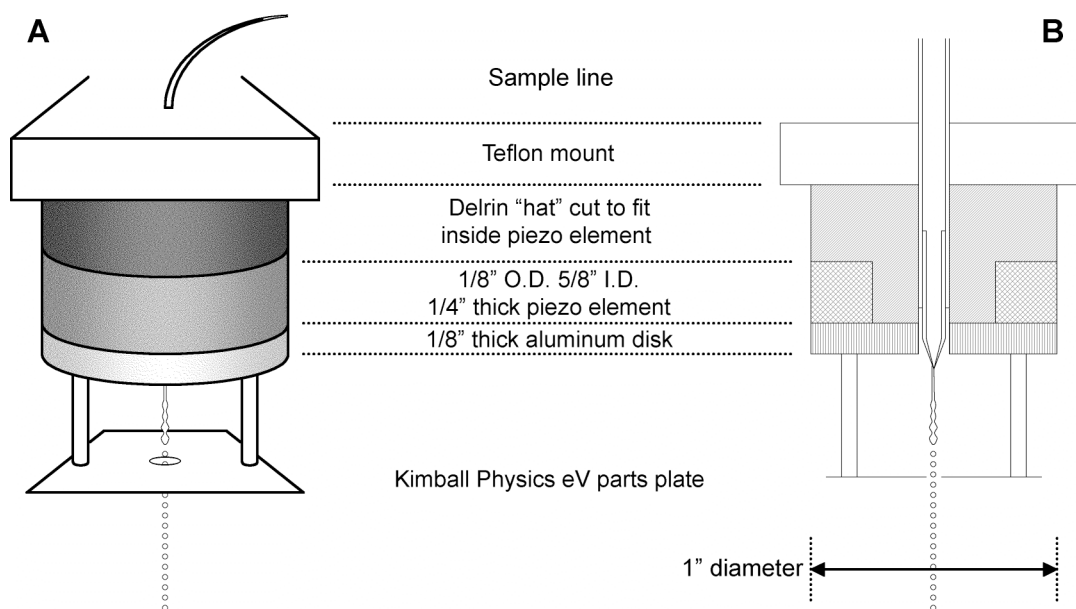
Kimball Physics eV parts plate

1" diameter

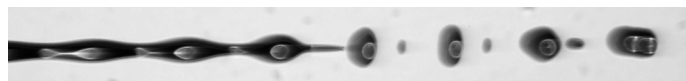Figure B.2. Perspective (A) and cutaway (B) drawing of the VOAG source.

Figure B.3. Capillary instability and droplet formation guided by a vibrating orifice. Primary droplets are 225 μm and are accompanied by smaller satellite droplets.

The 5 V TTL output of a Pentek model 3100 digital frequency synthesizer provides this square wave. The orifice diameter and solution flow rate establish a natural breakup frequency between 9 and 11 kHz for methanol. One side of the piezo element is electrically connected to the aluminum disk which is set at a voltage V_c discussed in section B.2.2. As a result, the square wave must float at V_c and is correspondingly passed through an optoisolator circuit discussed in section B.3.1.

Figure B.3 shows a flashlamp-illuminated image of stream breakup and droplet formation. The stream clearly shows a wave superimposed on the column of liquid prior to breakup. Breakup results both 225 μm methanol droplets and smaller satellite droplets common to vibrating aerosol generators. The droplets move at ballistic speeds with little drag because the air column between the droplets roughly travels along with the droplets.

B.2.2. Generating charged droplets

In an electric-field free environment, droplets produced by a VOAG show a small statistical charge distribution on the order of hundreds of elementary charges. Establishing an electric field in the region where droplets break off of the liquid column allows us to control the net charge on the droplets. In our design, this is accomplished by connecting both the methanol sample line and the aluminum plate to a voltage supply V_c and placing a grounded plate below the point at which the stream breaks into droplets. As shown in Figure B.2, this plate is set 1 cm off of the aluminum disk through the use of nylon screws and ceramic spacers. The voltage V_c was varied between 0 and 600 V resulting in droplets with charge as high as 13% of their Rayleigh limit.

Higher voltages and charges closer to the Rayleigh limit are experimentally attainable but not practical for our dynamics experiment. This is attained by either increasing V_c or by allowing the droplets to evaporate to a higher charge density. At higher charge values, space-charge repulsion between the droplets causes radial movement beyond the droplet stream. This results in a fine mist unsuitable for the experiment. Future experiments could explore the impact of higher droplet charge by using a different technique to generate charged droplets, or by selecting a small number of droplets from the charged droplet "mist".

B.3. Electric circuits employed in the dynamics experiment

B.3.1. Optoisolator circuits

Optoisolators employ a light emitting diode (LED) to switch a phototransistor within a single, sealed package. Signals are transferred through the LED-phototransistor pair, but cannot go the other way. This has two applications, both of which are employed in the dynamics experiment. Firstly, the input signal is isolated from electrical noise generated by devices connected to the optoisolator output. Noise cannot be transferred back to the controlling circuitry. Secondly, the output stage may be set at a completely different reference voltage than the input stage. Thus signals may be "floated" or sent to a device with a different ground than the controlling circuit.

Figure B.4A shows the schematic configuration of the optoisolators employed in the dynamics experiment. The optoisolator itself is either a 6N135 or an HCPL-4502 which are functionally identical used interchangeably. The LED side contains a 47 ohm resistor that current-limits the incoming signal. The phototransistor is wired in an

emitter-follower configuration such that the shape of the output pulse directly mimics the input pulse. A 6V lantern battery supplies the for the output pulse.

In cases where the optoisolator serves to isolate a signal due to electrical noise concerns, the floating high voltage (HV) input is wired to the same ground as the input signal. In cases where the output pulse is floating relative to HV, that voltage is wired to the "floating HV or ground in" connection. As an example, an optoisolator delivers the square wave signal to the piezoelectric actuator in the VOAG. The square wave input is a TTL signal and the output signal is a 6V square wave relative to V_c.

Because this circuit is used often in these experiments, the circuit is designed to be modular and inserted between sources and devices where necessary. In schematics presented later in this chapter, this circuit is approximated by the shorthand notation shown in Figure B.4B.

B.3.2. Synchronization of switched fields and droplet generation

High speed photography of droplets exposed to a high field for a specified period of time requires precision synchronization of field switching, flashlamp firing, and VOAG frequency. Figure B.5 illustrates the pulse sequences within the dynamics experiment. The high voltage and flashlamp control electronics trigger off of the VOAG square wave (Figure B.5A), which is a 5V TTL signal that oscillates at ν_{VOAG}. The square wave signal passes through two "decade" counters that generate square waves of frequencies $\nu_{VOAG} \div 10$ (Figure B.5B) and $\nu_{VOAG} \div 100$ (Figure B.5C), respectively. The latter frequency is useful because it has a working period of approximately 10 ms. In this
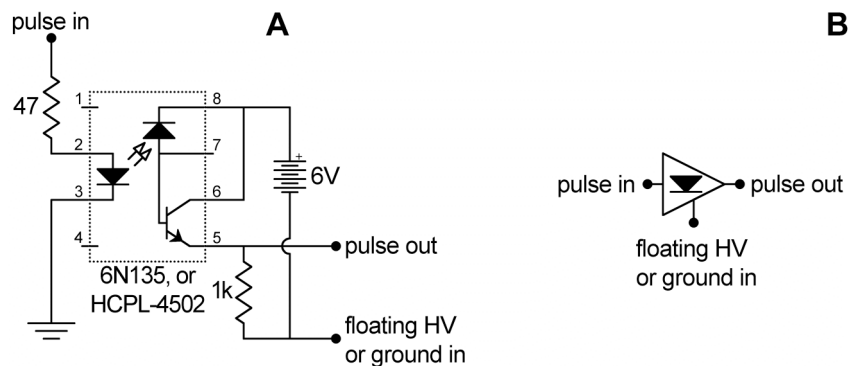
Figure B.4. Schematic diagram of the optoisolator circuit (A). All resistances are in ohms. Frame (B) shows a shorthand notation for this circuit used in other schematics.
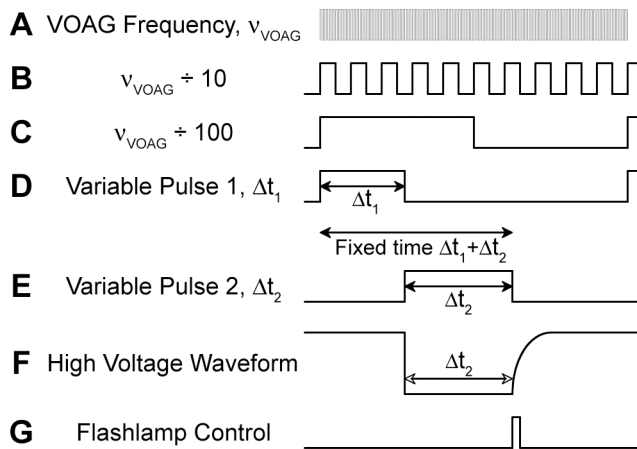

Figure B.5. Pulse sequence for the electronics in the dynamics experiment.

time, the high voltage electronics have plenty of time to switch on, establish a high electric field, switch off, and reset before another period begins.

Two timing pulses set the duration of the high voltage pulse. As shown in Figure B.5D and E, the length of these pulses is variable but the sum of their time lengths remains constant. The high voltage waveform (Figure B.5F) mirrors the second variable pulse, and the flashlamp (Figure B.5G) triggers on the downswing of the second variable pulse, or at the end of Δt_2. In this configuration the timescale of the high voltage waveform is variable, however it always ends at the same time relative to the VOAG frequencies. As a result, the flashlamp always fires in phase with the VOAG, and droplets are repeatedly visualized at a consistent physical location in space.

Figure B.6 shows a schematic diagram of the synchronization circuitry. The VOAG signal is directed into a series of two decade counters to generate the $\nu_{VOAG} \div 100$ signal in Figure B.5C. A 50 Ω resistor provides a low input impedance to match the output of the PENTEK. The $\nu_{VOAG} \div 100$ triggers two monostable vibrators in a single 74LS123 integrated circuit that generate the two variable pulses of Figure B.5D and E. Each pulse length Δt is cRC where R is an input resistance, C is an input capacitance, and c is a proportionality constant of the integrated circuit. For the two vibrators, the capacitors are each matched at 23 nF and one common 100 kΩ potentiometer (pot) sets the resistance. The variable connection to the pot is set at 5V and each terminal is connected to a vibrator; thus the variable connection changes the individual resistance however the total resistance remains constant. Since $\Delta t_1 = c R_1 C_1$, $\Delta t_2 = c R_2 C_2$, and $C_1 = C_2 \equiv C$; $\Delta t_1 + \Delta t_2 = cC(R_1 + R_2) = constant$ because $R_1 + R_2 = 100 k\Omega$. The second
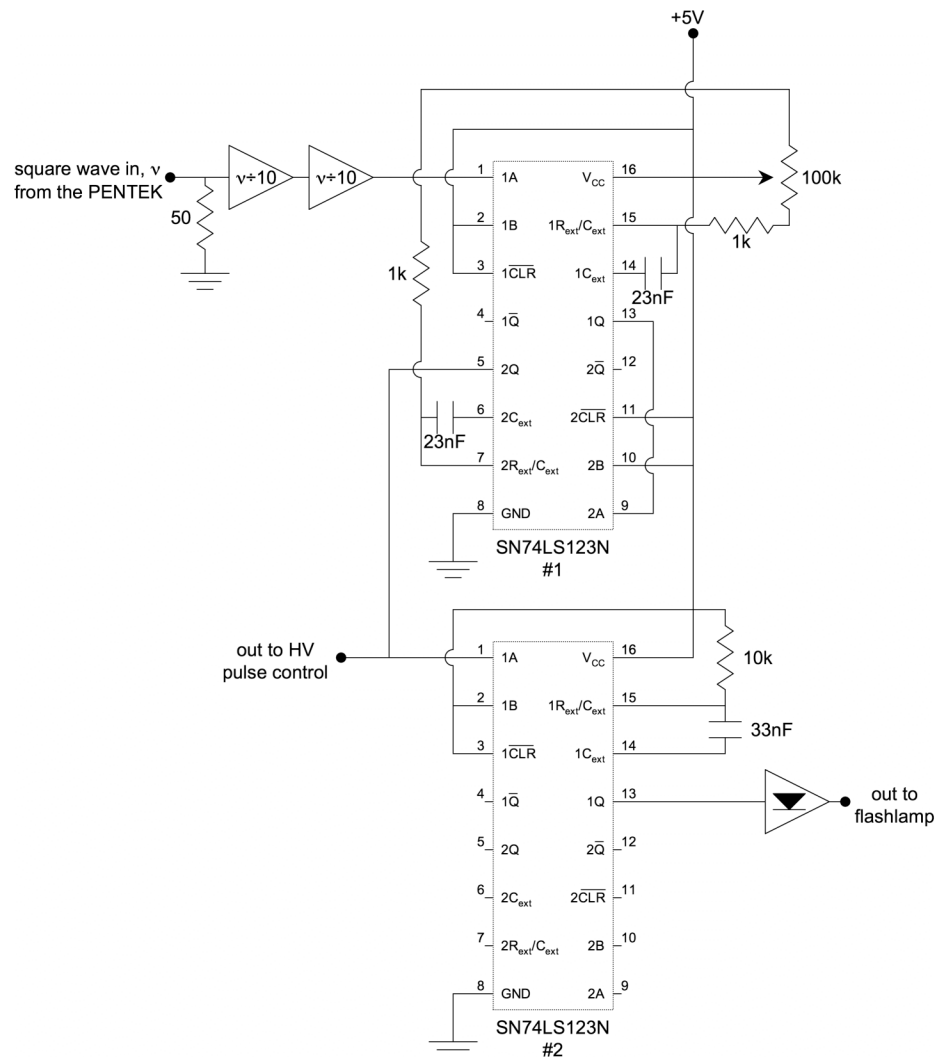
Figure B.6. Schematic diagram of the timing circuitry for the dynamics experiment. The VOAG square wave passes through two decade counters and triggers the 74LS123 monostable vibrators. The vibrators generate output pulses for the high voltage switch and the flashamp.

vibrator generates the control pulse for the high voltage switch discussed in the next section.

The second 74LS123 (#2 in Figure B.6) generates the flashlamp trigger based on the downswing or the end of the high voltage control pulse. The output signal from this vibrator passes through an optoisolator because the flashlamp generates significant electrical noise.

B.3.3. High voltage switching

Figure B.7 shows a schematic of the high voltage pulsing circuit. The HV pulse control from Figure B.6 is sent to four optoisolators. This signal passes through a single Schmitt trigger then breaks into four parallel signals that each pass through a second Schmitt trigger before controlling the optoisolators. In this configuration, the optoisolator driving current comes from the Schmitt triggers rather than the control pulse, and this provides convenient test points for circuit debugging.

Each optoisolator drives a single high voltage MTP1N100E 1kV switching MOSFET. The MOSFETS stack parallel to a chain of 4.7 MΩ resistors. The resistor network at the top of the figure consists of nine parallel 4.7 MΩ resistors in series with ten parallel 4.7 MΩ resistors. This arrangement provides an overall resistance of 1 MΩ, but the voltage drop across individual resistors is less than their 1 Watt rated power. The resistor chain configuration means that the maximum source-drain voltage is only $4.7 / (4.7 \times 4 + 1)$ or ~24% of the total voltage supplied. With a 4kV maximum input voltage provides a maximum switching peak-to-peak pulse of $(4.7 \times 4) / (4.7 \times 4 + 1)$ or ~3800 Volts.
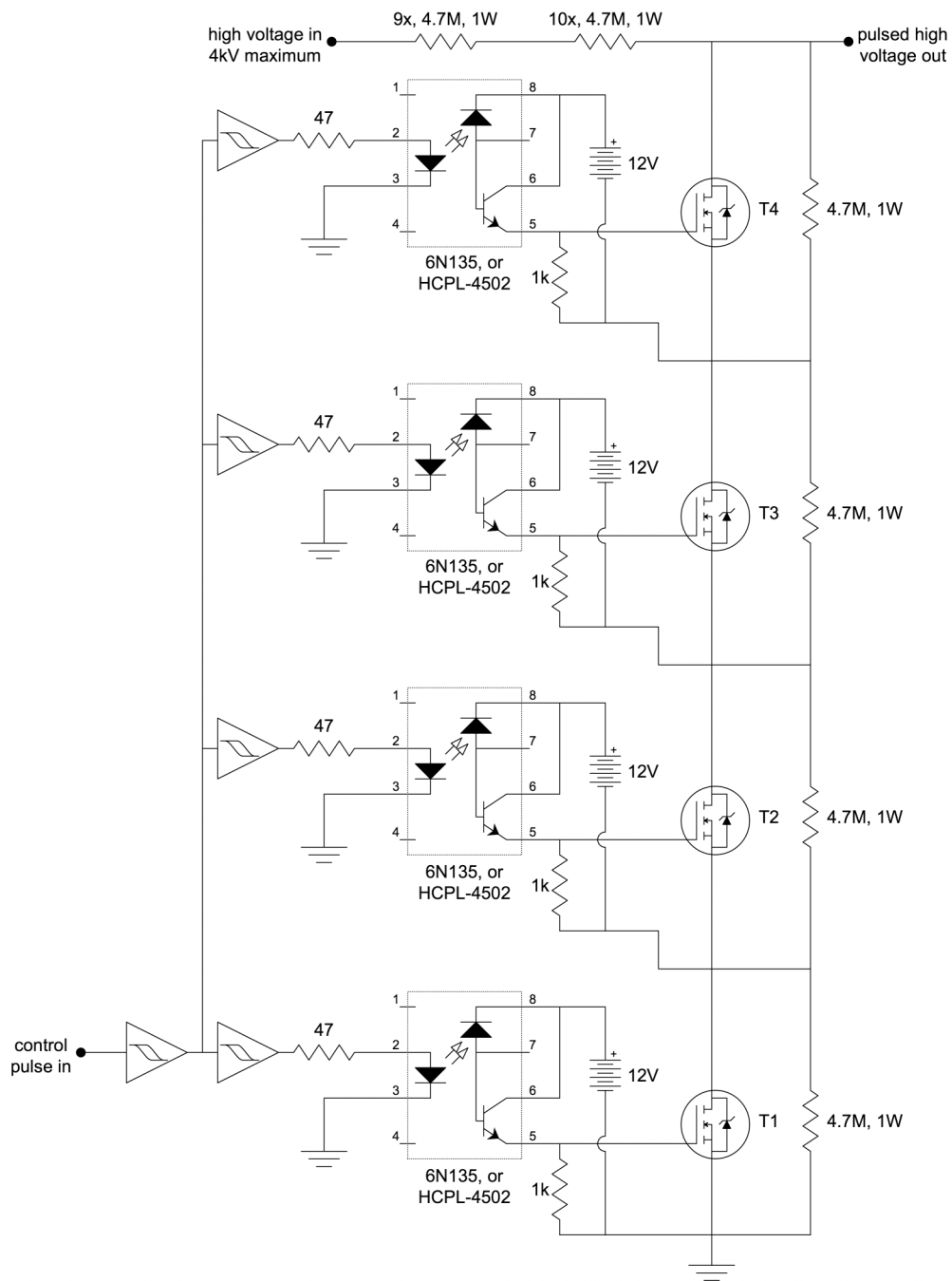
Figure B.7. High voltage pulsing circuit. A control pulse is sent to four optoisolators which each drive a high voltage MOSFET.

B.4. Conclusions and design considerations for future dynamics and FIDI-MS experiments

The FIDI dynamics experiment investigated the dynamics of FIDI using switched high electric fields to enable time-resolved studies of droplet distortion, Taylor cone formation, and charged progeny droplet extraction from neutral and charged 225 micron methanol droplets. Future work may explore this phenomenon on a wider range of solvents and droplet sizes considering the effect of analytes and binary solutions. Additionally, we noted a relationship between the timescale of FIDI and the frequency of shape oscillations that occur below the Taylor limit. We explored this relationship through a single droplet oscillation period which future work may investigate over a longer timescale.

B.5. References

(1)   Grimm, R. L.; Beauchamp, J. L. *J. Phys. Chem. B* **2005**, *109*, 8244.

(2)   Chen, B. T.; John, W. Instrument Calibration. In *Aerosol Measurement: Principles, Techniques, and Applications*; Baron, P. A., Willeke, K., Eds.; Wiley-Interscience: New York, 2001; pp 627.